Fiber-Oriented Regularization of Diffusion Tensor Images

Y. Lu[1], J. Qi[2], A. Anderson[1], J. C. Gore[1], Z. Ding[1]

[1]The Institute of Imaging Science, Vanderbilt University, Nashville, TN, United States, [2]Radiology, The First Affiliated Hospital of Nanjing Medical University, Nanjing, China, People's Republic of

Introduction

Diffusion tensor regularization approaches have recently focused on boundary preservation during reduction of noise in diffusion tensor images [1-3]. However, since diffusion tensor images suffer from both noise and partial volume averaging (PVA), regularization approaches robust to PVA are called for. To meet this need, this study proposed a new regularization method that is based on a Bayesian framework and fiber-oriented regularization scheme. Experiments with synthetic data have demonstrated the superior performance of this technique in the presence of noise and PVA.

Methods

1. *Framework*: In noisy diffusion tensor imaging data, the diffusion tensor element vector $\boldsymbol{d} = (D_{11}\ D_{22}\ D_{33}\ D_{12}\ D_{13}\ D_{23})$ at each voxel is assumed to be a multivariate normal distribution: $\boldsymbol{d} \sim N(\boldsymbol{\mu}, \boldsymbol{\Sigma})$, where D_{ij} is the element of diffusion tensor matrix (i, j = 1,2,3), $\boldsymbol{\mu}$ represents the unknown true tensor element vector, and $\boldsymbol{\Sigma}$ is the covariance matrix. The Bayes decision in tensor regularization is to determine the value of $\boldsymbol{\mu}$ that maximizes the *a posteriori* (MAP) probability $P(\boldsymbol{\mu}_j|\boldsymbol{d})$, which is the product of the conditional probability density $p(\boldsymbol{d}|\boldsymbol{\mu}_j)$ and the *a priori* probability $P(\boldsymbol{\mu}_j)$, i.e.:

$$\boldsymbol{\mu} = \underset{\boldsymbol{\mu}_j}{\operatorname{argmax}}\,(P(\boldsymbol{\mu}_j|\boldsymbol{d})) = \underset{\boldsymbol{\mu}_j}{\operatorname{argmax}}\,(p(\boldsymbol{d}|\boldsymbol{\mu}_j)\cdot P(\boldsymbol{\mu}_j)/p(\boldsymbol{d})) = \underset{\boldsymbol{\mu}_j}{\operatorname{argmax}}\,(p(\boldsymbol{d}|\boldsymbol{\mu}_j)\cdot P(\boldsymbol{\mu}_j), j = 1, 2, ..., n)$$

Under the assumption of a multivariate normal distribution: $\boldsymbol{\mu}_j \sim N(\boldsymbol{m}, \boldsymbol{S})$, where $\boldsymbol{m}$ is the mean and $\boldsymbol{S}$ is the covariance matrix, $P(\boldsymbol{\mu}_j|\boldsymbol{d})$ still behaves normally, i.e., $P(\boldsymbol{\mu}_j|\boldsymbol{d}) \sim N(\hat{\boldsymbol{\mu}}, \boldsymbol{\Psi})$, where $\hat{\mu} = (\Sigma^{-1}+S^{-1})^{-1}(\Sigma^{-1}d+S^{-1}m), \Psi^{-1} = \Sigma^{-1}+S^{-1}$ [4]. Hence the MAP solution for tensor regularization has a mean value of $\boldsymbol{\mu} = \hat{\boldsymbol{\mu}}$ and a covariance matrix $\boldsymbol{\Psi} < \boldsymbol{\Sigma}$ or $\boldsymbol{S}$, giving an optimal estimation of the true tensor matrix with smaller uncertainty. $\boldsymbol{d}$ and $\boldsymbol{\Sigma}$ can be estimated directly from the measured diffusion weighted images [5], and $\boldsymbol{S}$ is estimated from a homogeneous high anisotropic region. Since $\boldsymbol{S}$ represents the uncertainty of underlying fibers, it can be assumed to be a constant for a specific data set. $\boldsymbol{m}$ is a fractional anisotropy (FA) weighted average of three consecutive tensor matrices (at previous, present and next voxels) along the propagating direction of a fiber. Fiber propagation is performed by the FACT fiber tracking method [6].

2. *Tests with synthetic data*: The synthetic data set was designed to contain anisotropic and isotropic regions, and a fiber crossing area as shown in Fig. 1(a). To mimic closely *in vivo* conditions, synthetic tensors were constructed to have a trace of $2.1*10^{-5}$ cm^2/s, and diffusion weighting was along six non-collinear directions with a *b* value of 1000 s/mm^2. Tensors for anisotropic regions were designed to be cylindrically symmetric ($\lambda_1 > \lambda_2 = \lambda_3$) with an identical eigenvalue contrast ($\Delta\lambda = \lambda_1 - \lambda_2 = 0.8*10^{-5}$ cm^2/s); tensors for isotropic regions and the fiber crossing area were isotropic ($\lambda_1 = \lambda_2 = \lambda_3$). The signal-to-noise ratio of this data set was 20, and the data size was 10*10*5 voxels. $\boldsymbol{S}$ was estimated from a homogeneous region with high FA as shown in the bottom blue rectangle in Fig. 1(a). Tensor regularization was started from two different seed regions and propagated until some termination criteria were met (e.g. out of boundary, sharp turn, etc.).

3. *Performance evaluation*: The mean absolute difference between the regularized tensor matrices $\boldsymbol{D_r}$ and true tensor matrices $\boldsymbol{D_0}$ was defined to be the index for measuring the performance of tensor regularization: $\delta = \frac{1}{N}\sum_{p=1}^{N}\sum_{i,j=1}^{3} | D_{r,ij}{}^{p} - D_{0,ij}{}^{p} |$, where N is the total number of regularized voxels. For performance comparisons, a Gaussian smoothing method (kernel size = 5*5*5, variance = 1) and an anisotropic smoothing method [2] (iterations = 70) were used.

Results

Figure 1 shows the regularization results with synthetic data using the three regularization methods mentioned above. Fig. 1(b-d) and (f-h) respectively show the results from the start region I and II (red: Bayesian; green: Gaussian; blue: anisotropic), which are superimposed on the original noisy tensor field. Fig. 1(e) shows the index δ with no smoothing and with smoothing by the three methods. It can be seen that the Bayesian method performs best not only in noise reduction, but in boundary preservation as well. Particularly in the PVA region it outperforms the other two methods and recovers the true fiber orientation.

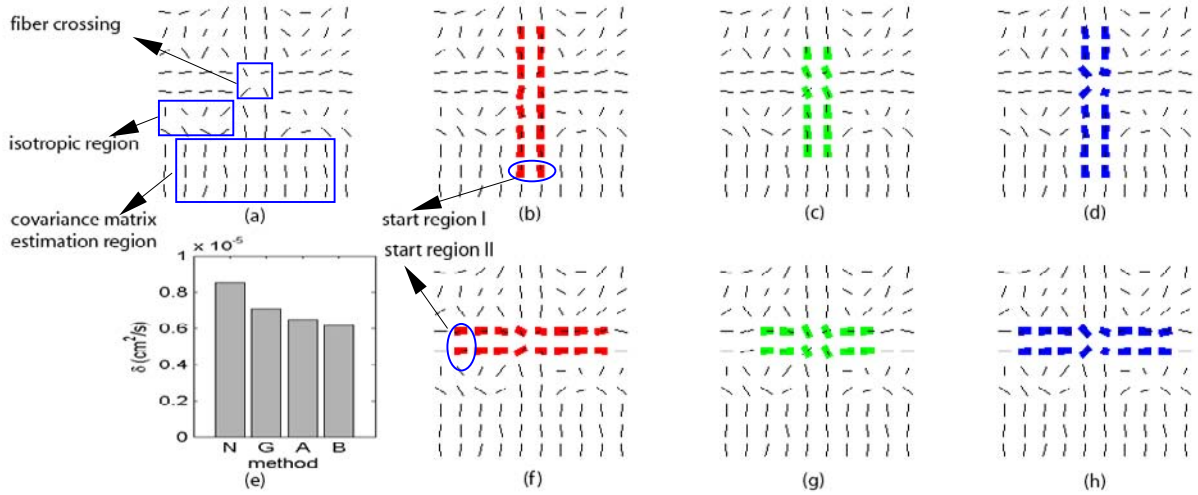

Figure 1. Regularization results with synthetic data: (a) the noisy tensor field with line segments indicating the directions of the major eigenvector. (b-d) results from the start region I by the Bayesian (b), Gaussian (c), and anisotropic (d) method. (f-h) results from the start region II with the three methods respectively. (e) performance measure δ with and without smoothing (N: no smoothing; G: Gaussian; A: anisotropic; B: Bayesian).

Discussion and conclusion

This study has demonstrated that the new approach has a superior performance of noise reduction, boundary preservation, and PVA robustness in regularizing diffusion tensor images. However, it still needs improvements to resolve larger PVA regions and more complex PVA patterns due to such as fiber kissing, branching, etc. Performance evaluation and method comparisons using *in vivo* human tensor data will be made in the future.

References [1] Parker GJM, et al., JMRI 2000:11:702-710. [2] Ding Z, et al., MRM 2005:53: 485-490. [3] Chen B, et al., MRM 2005:54:393–401. [4] Lu Y et al., NeuroImage 2005 (submitted). [5] Anderson A, et al., MRM 2001:46: 1174–1188. [6] Mori S, et al., Annals of Neurology 1999:45:265–269.